WELDING RESEARCH

SUPPLEMENT TO THE *WELDING JOURNAL*, NOVEMBER 1987

Sponsored by the American Welding Society and the Welding Research Council

An Analytical Model for Laser Reflow Soldering of an Electronic Component

Analytic predictions of solder joint integrity are in good agreement with observations from an actual application

BY D. U. CHANG

ABSTRACT. An analytical model for laser reflow soldering of a thick-film ignition module is presented in this paper. The analytical model is used to better understand the effect of process variables on soldering. The process variables investigated include beam power, beam on-time, beam spot diameter, preheat temperature, and specimen materials and configurations. Conclusions drawn from the model analysis are compared against experimental results for verification. The model was found useful in understanding the process and developing an optimum soldering schedule for manufacturing.

Introduction

Lasers provide high-intensity, controllable sources of heat for material processing, ranging from heat treating to welding and cutting. Successful applications (Refs. 1–8) are characterized by unique advantages of the laser such as precision, excellent product quality, high productivity, low manufacturing cost and easy automation.

D. U. CHANG is with Lasertech, Inc., Windermere, Fla., a laser applications consulting company.

Even with these advantages, a good understanding of the process variables and their effects is necessary before a potential application can be successfully implemented. An analytical model would be helpful in this regard.

This paper presents an analytical model that can be used in laser soldering studies for better understanding and control of the process. The intention of this paper is not to present an exhaustive experimental soldering study, but to present an example of how an analytical model can be used effectively to understand the process for better design, control and manufacture of particular components.

KEY WORDS

Alumina Substrate
Beryllia Substrate
c-radius Equation
Ignition Module
Reflow Soldering
Melting Efficiency
Power vs. Time
Thermal Radius
Thick-Film Circuit
Analytical Model

The particular process under investigation was laser reflow soldering of a thick-film ignition module — Fig. 1.

A summary of the previous experimental results will be presented first. Then, the critical thermal radius concept (Ref. 9) developed earlier will be expanded for use in the analysis of the effect of beam power, beam on-time, beam spot diameter, preheat temperature and other process variables, as well as the materials' thermal properties. Comparisons will be made between analytical predictions and actual experimental data to assess the validity of the model. Lastly, the usefulness of the model will be discussed.

Results of Previous Experiment

Presented below is the summary of an experimental investigation of laser reflow soldering for joining electrical leads to printed circuits of an automotive electronic component (Ref. 3).

Specimen

The specimen was an electronic module, with nine terminal leads, which was to be soldered to a hybrid thick-film circuit — Fig. 1. Eight leads were to be joined to solder pads on an alumina

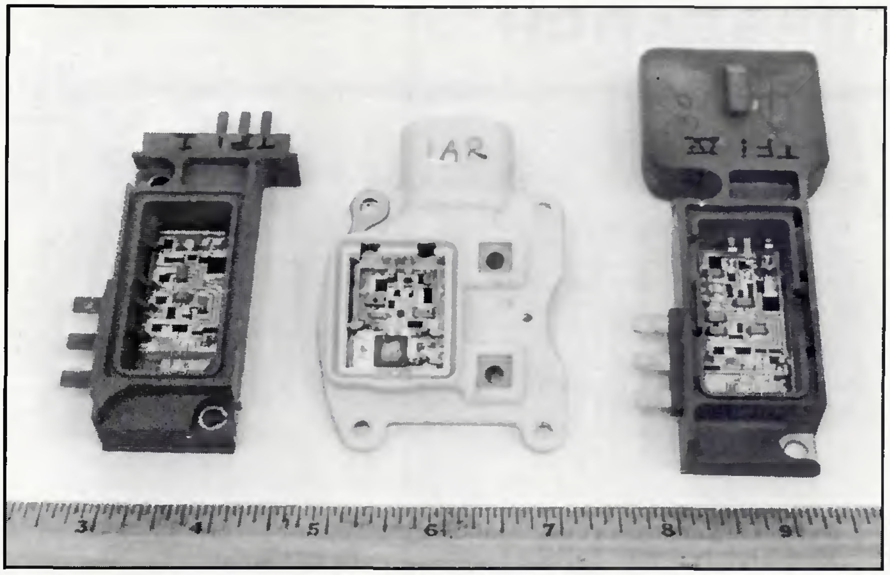

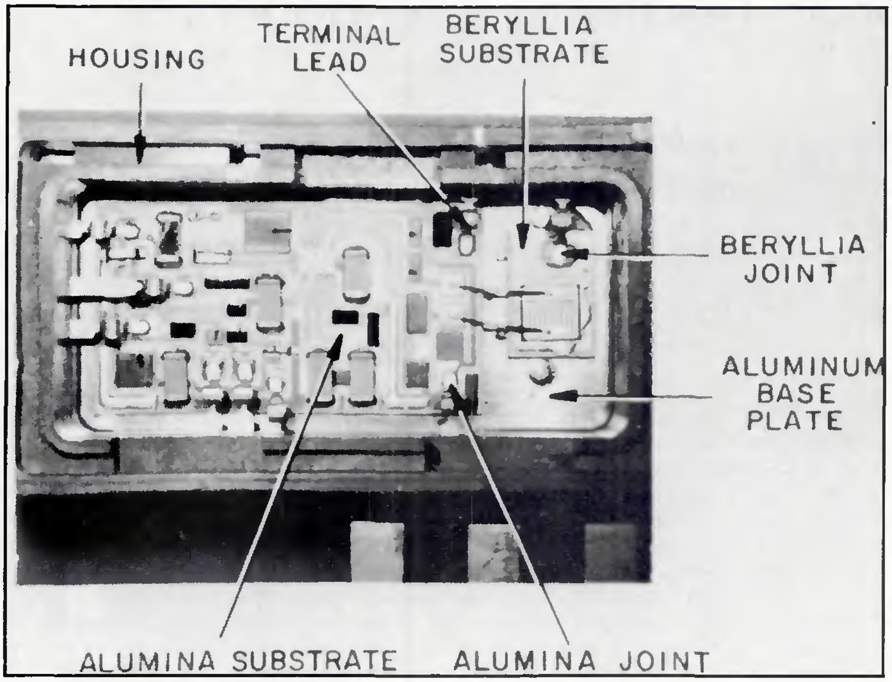

Fig. 1 — Thick-film ignition module

substrate and one to a solder pad on a beryllia substrate.

A cross-section through a terminal lead is shown in Fig. 2. The dimensions and compositions of the terminal lead and the solder pad are shown in Table 1.

Procedure

A defocused laser beam (a beam some distance after the focal point) from a 375-W CO_2 laser was impinged on the lead/solder pad area to effect laser soldering. The mode structure of the output beam of this laser is expected to be 95% in TEM_{oo} (Ref. 9).

Unless otherwise mentioned, the test conditions listed in Table 2 prevailed.

Table 1—Specimen Data

Part Name	Thick-Film Ignition Module – IV
Materials	(See Fig. 2)
Terminal Lead	SAE CA 260 brass, ½ hard, 0.040 in. wide × 0.009 in. thick, tin-plated. Nominal composition is 70% Cu-30% Zn. The end is semicircular in shape with a 0.020-in. radius.
Solder Pad	10Sn-88Pb-2Ag, 0.080 × 0.100 × 0.006 in. thick.
Alumina Substrate	94% nominal Al_2O_3, 0.022 in. thick
Beryllia Substrate	99.5% minimum of BeO, 0.022 in. thick
Aluminum Base Plate	AA 3003-H14, 0.060 in. thick

Power vs. Time

As the beam on-time increased at a given power level, the following sequence of the joint formation was noted: 1) "sticking," which indicated the onset of soldering – Fig. 3A; 2) "fillet forming," where the separation line between the terminal lead and the solder pad disappeared and a fillet started to form – Fig. 3B; and 3) "satisfactory fillet," where a smooth solder fillet was formed around the terminal lead for positive indication of soldering – Fig. 3C. As the time increased, more solder area melted "good fillet" – Fig. 3D). Excessively long times melted the terminal lead and the substrate, thus resulting in a defective solder joint. The beam on-times for sticking, fillet forming, and satisfactory fillet conditions are shown in Table 3.

Review and Expansion of Analytical Model

Critical Thermal Radius

The critical thermal radius (c-radius) is the radius (or width, in the case of a moving heat source) of an area where the desired thermal effect has been accomplished (Ref. 9).

The particular c-radius selected in this analysis was the melt radius on a solder pad. A thermal analysis of the workpiece and the spatial distribution analysis of the beam led to an expression of the c-radius in terms of characteristic beam spot diameter, beam power, surface absorptivity, thermal resistance, specific heats and densities of materials, laser beam on-time, melting point of the solder and the specimen temperature. A simple thermal model of one-dimensional heating was assumed in the analysis.

The thermal analysis was performed on the lumped subsystems rather than on the continuance of the multilayer specimen as shown in Fig. 2. The lumped approach greatly simplified the analysis and has been proven effective.

The c-radius equation for the present specimen configuration and a Gaussian beam of the $1/e^2$ radius, a, is (from Ref. 9):

$$c = \frac{a}{\sqrt{2}}\left[\ln\left(2PAR\left[1 - \exp\left(-\frac{0.975t}{RC}\right)\right]\right) \Big/ \pi a^2 (T_m - T_o) \right]^{1/2} \quad (1)$$

where

c = critical thermal radius (radius of solder melt area).

a = beam spot radius @ $1/e^2$.
P = beam power.
A = surface absorptivity.
R = thermal resistance from the solder pad to the aluminum heat sink.
C = heat capacity.
t = beam on-time.
T_m = melting point of the solder.
T_o = specimen temperature or preheat temperature.

Substitution of appropriate conversion factors and the melting point temperature of the solder (Tm = 320°C) into Equation 1 yields

$$c = \frac{a}{\sqrt{2}}\left[\ln\left(0.02359\,W\,A\,R\left[1 - \exp\left(-\frac{0.975t}{RC}\right)\right]\right) \Big/ a^2\,(320 - T_o)\right]^{1/2} \quad (2)$$

The units of the parameters are: c = (in.), a = (in.), W = (watt), A = (% ÷ 100), R = (°C/s cm^2/cal), t = (s), C = (cal/°C cm^2), and T_o = (°C).

Here

$$C = C_1 + \frac{C_2}{3} \quad (3)$$

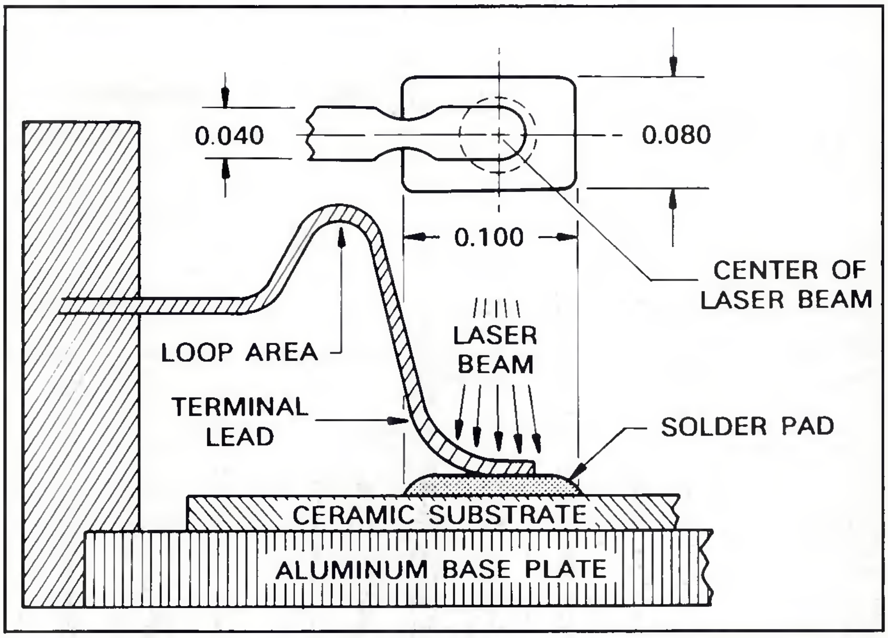

Fig. 2—Solder joint configuration (in.)

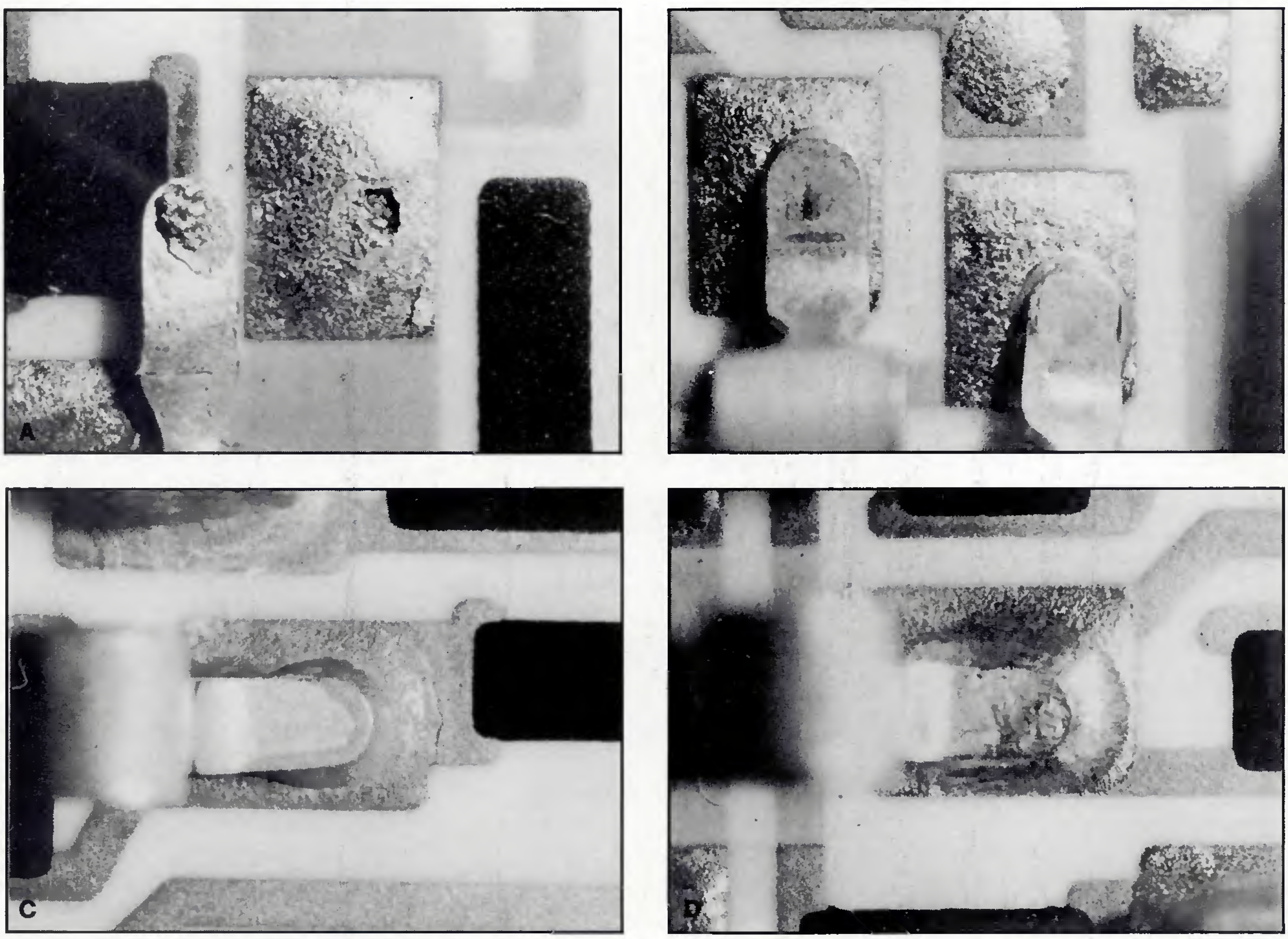

Fig. 3—Progressive states of solder joint formation. A—Sticking; B—fillet forming; C—satisfactory fillet; D—good fillet (typical)

Table 2—Test Conditions

Beam Spot Diameter	0.060 in. @ $1/e^2$ after focal point
Preheat Temperature	150°C
Shielding and Blow-off Gas	N_2
Flux	Nonactivated rosin microflux 5003
Terminal Lead/Solder Pad Contact	0.030 in. vertical deflection of the lead (corresponding contacting force ranged from approximately 50 g to 150 g, depending on the length of the terminal leads.)

Table 3—Soldering Schedule for Various Joints

Alumina Joints		Minimum Beam On-Time (s)			
		Power Level			
Joint Conditions	Preheat Temp. (°C)	100 W	200 W	300 W	400 W
Sticking	20	0.080	0.030	0.017	–
	150	0.030	0.012	0.006	–
Fillet Forming	20	0.60	0.060	0.035	–
	150	0.060	0.020	0.010	–
Satisfactory Fillet	20	1.0	0.12	0.050	–
	150	0.150	0.040	0.020	–
Beryllia Joints					
Sticking	20	–	–	–	–
	150	–	0.012	0.006	–
Fillet Forming	20	–	–	–	–
	150	>2.0	0.070	0.015	–
Satisfactory Fillet	20	–	≫2.0	>1.0	>1.0
	150	≫2.0	0.15	0.050	–

where

$$C_1 = c_1\rho_2 V_1 \quad (4)$$

$$C_2 = c_2\rho_2 V_2 \quad (5)$$

where

c_1, c_2 = specific heat of the solder and the ceramic substrate, respectively (cal/gm °C).

ρ_1, ρ_2 = density of the solder and the ceramic substrate, respectively (gm/cm^3).

V_1, V_2 = volume of the solder and the ceramic substrate on a unit area, respectively (cm^3/cm^2).

The units of parameters were selected for practical convenience in the usage of the equation, although the units are mixed. The product RC is the thermal time constant τ (s) of the system (workpiece)

$$\tau = RC. \quad (6)$$

c-Radius for Alumina Joints

The specific c-radius equation for alumina joints (solder joints on alumina substrate) could be obtained by calculating the heat capacity C. (See Appendix 1 for material properties.)

$$C = 0.01964\ (cal/°C\ cm^2)$$

The value of R was calculated to be 3.5 (°C s cm^2/cal) (Ref. 9). Therefore, the c-radius for the alumina joints is now

$$c = \frac{a}{\sqrt{2}}\left[\ln\left(0.08257\ W\ A\ [1 - \exp\left(-\frac{t}{0.0708}\right)]\right) \Big/ a^2(320 - T_o)\right]^{1/2} \quad (7)$$

and the thermal time constant is τ = 0.069 (s).

c-Radius for Beryllia Joints

The solder joints on the beryllia substrate would require more power than those on the alumina substrate, due to the higher rate of heat dissipation through the beryllia. In order to obtain a c-radius expression, the calculation of C and R of the beryllia substrate sample was necessary. The calculated values were:

R = 1.14 (C sec cm^2/cal)
C = 0.01875 (cal/°C cm^2)

Therefore

τ = RC = 0.021 (s)

and

$$c = \frac{a}{\sqrt{2}}\left[\ln\left(0.02689\ W\ A\ [1 - \exp\left(-\frac{t}{0.0215}\right)]\right) \Big/ a^2(320 - T_o)\right]^{1/2} \quad (8)$$

Analysis and Discussion

Solder Joint Condition vs. c-Radius

As shown in Fig. 3, the different solder joint conditions were related to the size of the solder melt area. If the diameter of the solder melt area was less than the width of the terminal lead (0.040 in./1 mm), a sticking condition occurred. When the diameter grew to the width of the lead, the interface line between the lead and the solder pad disappeared and a fillet forming condition resulted. If the melt area was large enough, a smooth fillet formed around the lead for a satisfactory fillet condition.

To compare the above solder joint conditions with the theoretical predictions, Equation 7 was plotted along with the experimental data for alumina joints shown in Table 3. Figure 4 shows the comparison for alumina joints which were preheated to 150°C (302°F). The solid lines indicate the calculated c-radii at a different power level, and the data points represent the beam-power/beam on-time combinations for sticking (S), fillet forming (FF), and satisfactory fillet (SF) conditions.

As shown, the satisfactory fillet condition occurred when the c-radius was approximately 0.026 in. (0.6 mm). In other words, if the c-radius was larger than one-half width (0.020 in./0.5 mm) of the terminal lead by 0.006 in. (0.15 mm) or more, a satisfactory fillet resulted. The fillet forming condition occurred when the c-radius was approximately 0.021 in. (0.53 mm), and the sticking condition occurred when the c-radius was less than 0.020 in. — one-half width of the terminal lead.

Figure 5 shows the three joint conditions for 20°C (68°F) alumina specimens. Again, the SF condition occurred when the c-radius was approximately 0.026 in. and the S condition occurred when the c-radius was less than one-half of the width (0.020 in.) of the terminal lead. The FF condition occurred at somewhat larger c-radius, as compared to 150°C specimens.

Beryllia specimen data (Table 3) were plotted in Fig. 6, which shows that the similar values of the c-radius signify the three joint conditions. Figure 7 is for 20°C beryllia specimens. Because of an insufficient number of available beryllia specimens, the room temperature (20°C) test could not be performed for comparison with the calculated c-radii. However, Fig. 7 may be useful in selecting proper parameters for room temperature beryllia specimens. It shows that room temperature beryllia specimens may not be soldered satisfactorily with a power level of 300 W or lower (as shown in Table 3).

Figures 4–6 show that the c-radius Equations 7 and 8 can be used to predict the solder joint condition, which is related to the area of melted solder. Conversely, values of the process variables (soldering schedule) can be calculated from the equations for the desired solder joint conditions.

Effect of Preheating

Initially, the specimens were preheated to eliminate any possibilities of thermal shock cracking of the ceramic substrates. Later, it was found that the preheating lowered the beam power requirement, as well as prevented thermal cracking (Ref. 3).

The reduced power requirement for a preheated sample may be calculated by using Equation 9, which was obtained by a simple manipulation of Equation 1.

$$\frac{W_2}{W_1} = \frac{320 - T_{o2}}{320 - T_{o1}} \qquad (9)$$

where

W_1 = power for specimen at temperature T_{o1}.

W_2 = power for specimen at temperature T_{o2}.

Equation 9 assumes that the beam on-time is constant.

The above relationship is shown graphically in Fig. 8, which indicates that a 150°C specimen will reduce the power requirement by 43%, as compared to a room temperature (20°C) specimen. A limited experiment showed that a 150°C specimen reduced the power requirement by 33%.

When the power is kept constant, a lower preheating temperature will require a longer beam on-time to effect the same soldering result. The beam on-time, t_2, for a specimen at a temperature, T_{o2}, is (from Equation 7)

$$t_2 = 0.0708 \ln\left[\frac{W_1 (320 - T_{o2})}{W_2 (320 - T_{o1})} \left[\exp\left[\frac{-t_1}{0.0708}\right] - 1\right]\right]^{-1} \qquad (10)$$

where

t_1 = beam on-time required for specimen at temperature T_{o1}.

t_2 = beam on-time required for specimen at temperature T_{o2}.

To check the validity of the relationship, calculated values of beam on-time were compared with experimental data, as shown in Table 4. The data in the column under "150°C Specimen (Measured)" were used to calculate the values in the next column, which were compared with experimental data in the last column. They were found to be in reasonable agreement, as shown in the last two columns of Table 4.

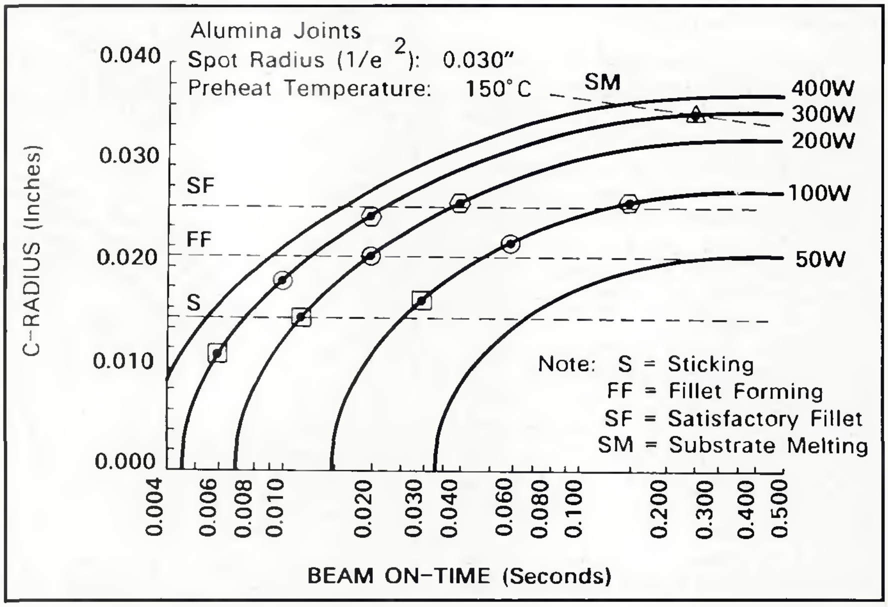

Fig. 4—c-radius as a function of beam power and beam on-time for alumina joints preheated to 150°C

Table 4—Effect of Preheat Temperature on Beam On-Time for Alumina Joints

Joint Condition	Power (W)	150°C Specimen (Measured)[a]	20°C Specimen (Calculated)	20°C Specimen (Measured)[a]
Sticking	100	0.030	0.075	0.080
	200	—	0.025	0.030
	300	—	0.016	0.017
Fillet Forming	100	0.060	(b)	0.60
	200	—	0.048	0.060
	300	—	0.027	0.035
Satisfactory Fillet	100	0.150	(b)	1.0
	200	—	0.095	0.120
	300	—	0.044	0.050

(a) Data from alumina joints, Table 3, basis for 20°C specimen calculation.
(b) Undetermined. The beam on-time is indefinitely long.

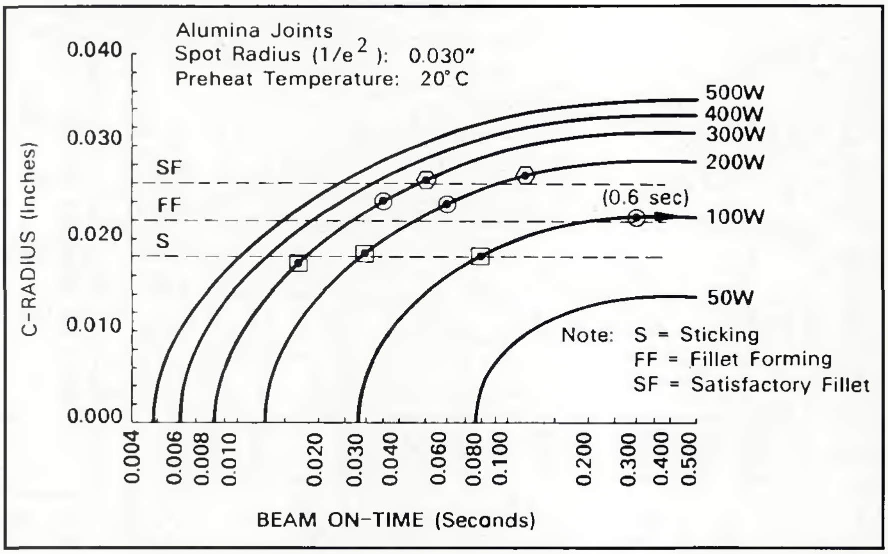

Fig. 5—c-radius as a function of beam power and beam on-time for alumina joints at room temperature

Effect of Beam Spot Diameter

The effect of beam spot diameter on c-radius (solder melt radius) is not as straightforward as the effect of other parameters. For a given power level, a small spot diameter gives an increase in power density, but at the same time, it limits the c-radius proportionally, due to the small beam spot diameter. These counteracting effects contribute to the complexity in predicting the beam spot diameter effect.

Equation 7 shows the relationship between the beam spot diameter (a) and the c-radius (c). The relationship is shown graphically in Fig. 9. At a relatively short beam on-time, a smaller beam spot produces a larger melt area. As the time gets longer, a larger spot diameter gives a larger melt area.

Figure 10 shows the effect of beam spot diameter on c-radius of the beryllia joints. Again, a larger spot diameter gives a smaller c-radius initially, but as the time extends, a larger spot diameter produces a larger molten area (a larger c-radius).

The selection of the beam spot diameter may depend on the desired melt radius (c-radius). The selected melt radius should be large enough to accommodate some beam/lead tip misalignment tolerance and still form a nice fillet around the entire periphery of the joint area.

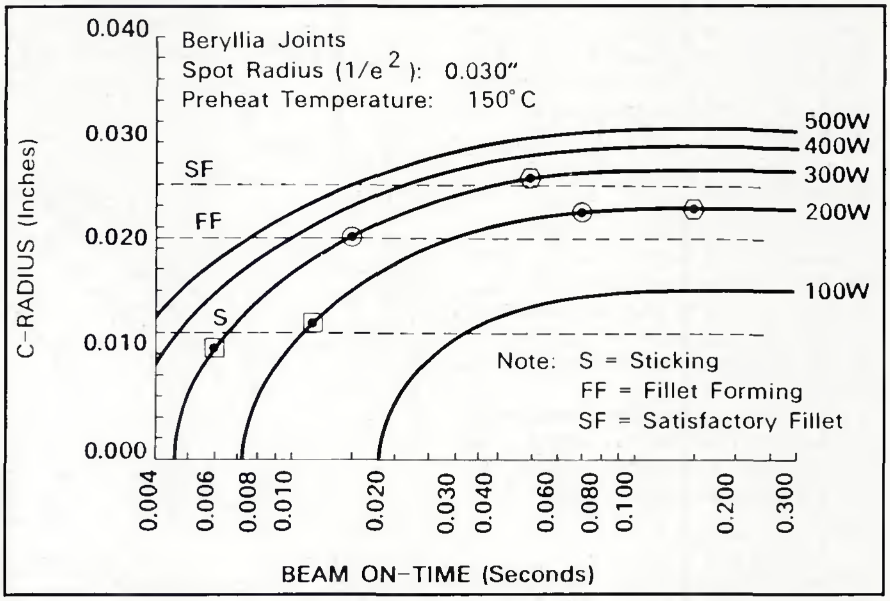

Fig. 6 — c-radius as a function of beam power and beam on-time for beryllia joints preheated to 150°C

Effect of Changes in Surface Absorptivity

Equation 1 indicates that the surface absorptivity increase has the same effect as the power increase.

$$A_1W_1 = A_2W_2 \tag{11}$$

where

A_1, A_2 = Surface absorptivity before and after surface modification.

W_1, W_2 = Power requirement before and after surface modification.

The surface absorptivity may be increased (or decreased) by modifying the surface condition of the workpiece. A common technique of increasing surface absorptivity is to apply an absorptive coating (such as black paint) on the surface.

Although no direct experiments were performed to quantify the relationship shown in Equation 11, some qualitative observations were made. The power requirements could be reduced substantially (on the order of 50%) by painting the lead surface black to increase the surface absorptivity (Ref. 3).

Temperature at the Terminal Lead/Solder Interface

The temperature at the terminal lead/solder interface is of particular interest because the bonding of a solder joint is strongly affected by this temperature. The interface temperature must be higher than the melting point (320°C/608°F) of the 10Sn-88Pb-2Ag solder to effect soldering, and yet should be lower than the melting point (775°C/1427°F) of the SAE CA260 brass terminal, because melting of the terminal lead is not desired.

The interface temperature should, therefore, be between 320°C and 775°C. Since the boiling point of the solder is 1740°C (3164°F), the solder under the terminal lead will not boil as

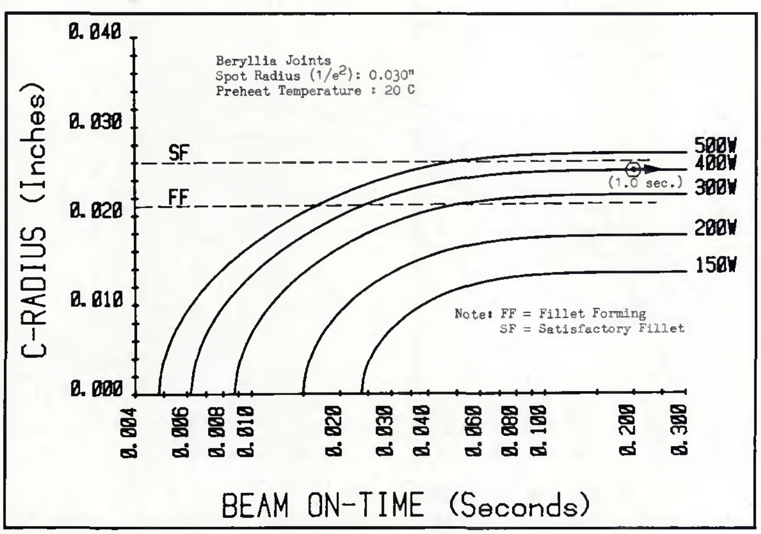

Fig. 7 — c-radius as a function of beam power and beam on-time for beryllia joints at room temperature

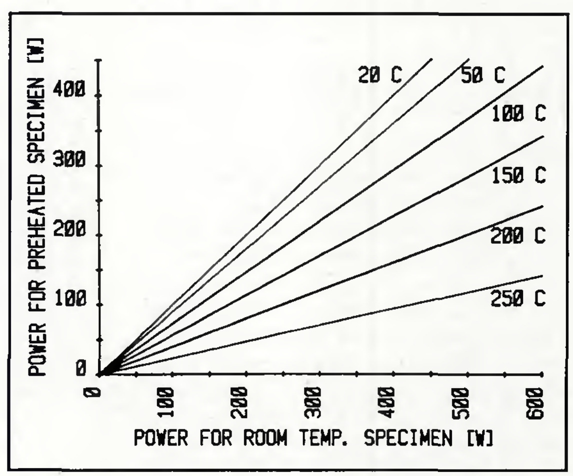

Fig. 8 — Effect of preheat temperature on power requirement

long as the terminal lead does not melt (*i.e.,* the porosity, if any, at the joint interface is not the result of solder boiling due to a high-intensity laser beam).

Thermal Resistance at the Terminal Lead/Solder Interface

The heat conduction through the interface of a terminal lead to a solder pad is directly affected by the thermal resistance at the interface.

If the heat input to the terminal lead is q, the thermal resistance of the terminal lead is R and that of the terminal lead/solder interface is R, as shown in Fig. 11, the energy balance of the system yields

$$q = C_t \frac{dT}{dt} + \frac{T}{R_t} + \frac{T}{R_i} \qquad (12)$$

where

- q = input heat flux.
- C_t = heat capacity of the tip area of the terminal lead.
- T = temperature of the tip area of the terminal lead.
- t = time.
- R_t = thermal resistance through the terminal lead extension.
- R_i = thermal resistance from the terminal lead to the solder.

The solution of the differential Equation 12 with the initial condition ($T = 0$ when $t = 0$) is

$$T = q\left(\frac{R_t R_i}{R_t + R_i}\right)$$

$$\left[1 - \exp - \left(\frac{t}{t_o}\right)\right] \qquad (13)$$

where

$$t_o = C_t\left(\frac{R_t R_i}{R_t + R_i}\right)$$

From Equation 13, one can calculate the safe heat input, which will not melt the terminal lead:

$$q < T_t\left(\frac{1}{R_t} + \frac{1}{R_i}\right)\frac{1}{\left[1 - \exp\left(-\frac{t}{t_o}\right)\right]} \qquad (14)$$

where

T_t = melting point of the terminal lead minus the specimen temperature.

Therefore, the thermal resistance R_i for nonmelting of the terminal lead, when the heat input is q and the time is t, is

$$R_i < \left[\frac{q_o}{T_t}\left[1 - \exp\left(-\frac{t_1}{t_o}\right)\right] - \frac{1}{R_t}\right]^{-1} \qquad (15)$$

where q_o is a given heat input.

The interface thermal resistance is dictated by the surface conditions at the interface and the contacting force (and possibly the contacting area as well). The required contacting force may be defined from the thermal resistance

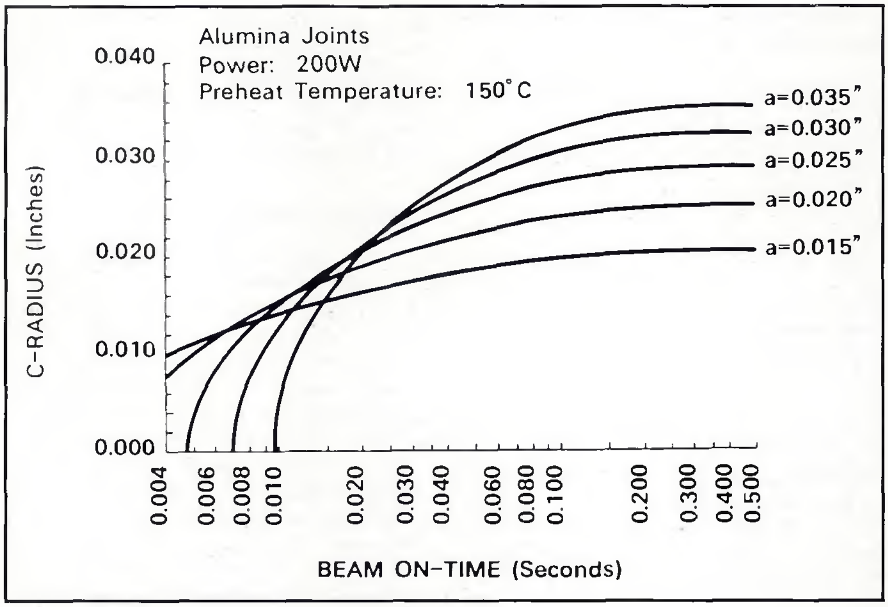

Fig. 9—Effect of beam spot diameter (= 2a) on c-radius for alumina joints

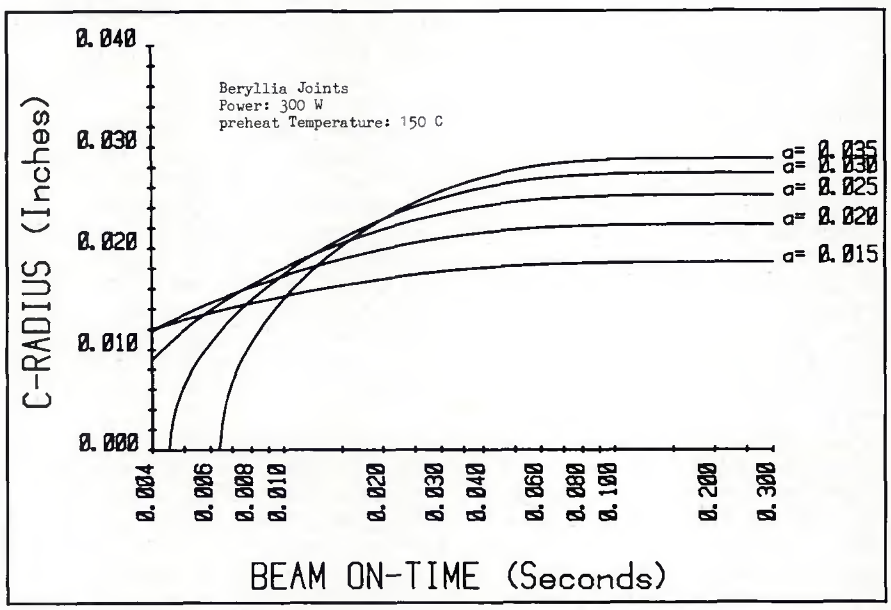

Fig. 10—Effect of beam spot diameter (= 2a) on c-radius for beryllia joints

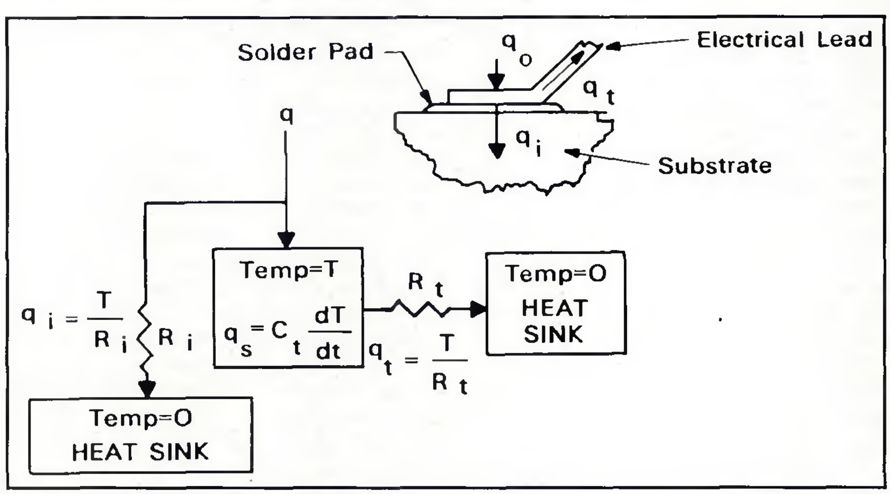

Fig. 11—Energy balance at the solder joint area

Table 5—Melt Efficiency in Laser Soldering

Power (W)	Joint Condition	Solder Melt Efficiency (%) 150°C Alumina	20°C Alumina	150°C Beryllia
100	FF[a]	11	2	—
100	SF[b]	8	2	—
200	FF	17	8	5
200	SF	14	6	4
300	FF	22	9	15
300	SF	19	10	8

(a) FF—Fillet forming condition.
(b) SF—Satisfactory fillet condition.

requirement once the surface conditions are determined.

It is interesting to note that laser soldering is a "stable" process. Once the interface temperature reaches the melting point, the molten solder bridges (wets) the interface between the lead and the alumina substrate and acts as a thermal coupling agent to effectively conduct the excess heat away from the terminal lead. This phenomenon may be responsible for a wide manufacturing window of this process (laser soldering), as exhibited in the earlier work (Ref. 3).

Melt Efficiency

The actual energy required to melt a certain volume of metal is usually much higher than the theoretical energy without any heat losses. The ratio of these energies, theoretical vs. actual, may be termed as the melt efficiency. This kind of ratio will be useful for a rough estimation of the energy requirement in a similar laser processing.

Table 5 shows the ratio of the theoretical and the actual energies to melt the solder (melt efficiency). The actual energies were calculated from the data in Table 3, with an assumption that the surface absorptivity is 10%. The theoretical energies are the energies needed to melt a volume of solder without heat loss.

As shown in Table 5, preheating allows an efficient use of the laser beam. Approximately 10 to 20% of the input heat energy was used to melt the solder on an alumina substrate when the specimen was preheated to 150°C. Room temperature alumina specimens showed only about 2 to 10% of the heat input usage rate. A higher melt efficiency was expected with a preheated specimen because preheating retards the cooling rate and thus reduces the rate of conduction loss.

Beryllia joints showed a low melt efficiency. This was expected because beryllia is a better heat conductor than alumina.

It was also evident that the solder melting efficiency decreased rather rapidly as the power decreased and the time increased. This may be explained by the fact that the conduction heat loss is approximately a parabolic function of the heating time, if one assumes that the solder temperature is a linear function of the heating time.

Summary and Conclusion

An analytical model of a laser reflow soldering process was presented in this paper. The general model was formulated previously by combining a one-dimensional heat conduction model and a spatial power density distribution (beam profile) model of a laser beam. The model, called the c-radius equation, allows calculation of a molten solder area as a function of process variables and thermal properties of the sample material for a few selected beam profiles.

The general model was reduced to suit the current specific application in this analysis. The application was a laser reflow soldering of thick-film hybrid electronic modules using a CO_2 laser beam with a TEM_{00} mode. The module had nine terminal leads to be soldered to printed circuits on alumina and beryllia substrates. Specific equations were developed to calculate the melt radii of the solder pads (Equations 7 and 8).

Experimental investigation showed that the solder melt area grew larger as the beam power and the beam on-time increased. "Sticking" occurred when the solder melt area was smaller than the terminal lead tip area, and a "satisfactory fillet" formed around the lead when the melt area was larger than the lead tip area.

The model was used to compare analytical predictions of solder joint quality (condition) to observed quality (condition). The prediction, which was based on the calculated radius of the molten solder area, was found to be in good agreement with the observation for the four different soldering situations studied.

The model also showed its usefulness in selecting process variables to obtain desired solder joint conditions (quality) without going through a time-consuming trial-and-error process of experimentation. The analytical method was especially useful when the available samples were too few to perform a meaningful experiment, such as the soldering of beryllia joints in this work.

The model was also found useful in evaluation of the effects of process variables. This process variable evaluation led to the following conclusions:

1) Preheating of the samples lowers the beam power requirement and/or shortens the beam on-time.

2) A large beam spot diameter does not necessarily produce a large melt area. When the power is low (and the beam on-time is short), a smaller melt area will result with a larger beam spot diameter.

3) Increasing the surface absorptivity is equivalent to increasing the beam power.

4) A high intensity laser beam does not boil solder, and it is not the cause of any porosity at the solder joint interface.

5) The contacting force at the joint interface should be high enough to conduct the heat to the solder pad without the excessive heat buildup at the terminal lead.

6) Only about 10% of the absorbed energy is used in direct melting of the solder. The energy usage rate (melt efficiency) improves if preheating is applied. A beryllia substrate is less efficient for melting solder pads than alumina substrate, probably due to its high thermal diffusivity.

Acknowledgment

This paper is based on work done at Ford Motor Company in 1982 by the author when he was a member of the research staff. The author is grateful to Ford Motor Company, especially the Electrical Electronic Division, for permission to publish the work.

References

1. Chang, U. I., and Casey, K. W. April 1979. Laser welding of exhaust gas oxygen sensor. Proceedings of a conference, *Applications of Lasers in Material Processing*. Washington, D.C., edited by E. A. Metzbower, published by ASM.

2. Chang, U. I. November 1981. Laser drilling of Pyrex glass for pressure sensor manufacturing. *Proceedings of First International Laser Processing Conference*, Anaheim, Calif.

3. Chang, D. U. 1986. Experimental investigation of laser soldering. *Welding Journal* 65(10):33–41.

4. Barber, R. B. Production application of CO_2 lasers. SME Report No. MR75-572.

5. Gresser, H. D. Laser sawing of diamonds. SME Report No. MR76-855.

6. Battista, A. D., and Shiner, W. H. Production laser hole drilling-now. SME Report No. MR76-861.

7. Anderson, D. G. Laser welding and cutting systems. SME Report No. MR76-856.

8. Bolin, S. R., and Maloney, E. T. Precision pulsed laser welding. SME Report No. MR75-571.

9. Chang, D. U. January 1983. Critical thermal radius in laser soldering. *Proceedings of Second International Conference on Applications of Lasers in Material Processing*. Sponsored by ASM International, Los Angeles, Calif.

10. Boltz and Tuve. 1970. *Handbook of Tables for Applied Engineering Science*. Chemical Rubber Co., Cleveland, Ohio.

11. Harper. 1969. *Handbook of Electronic Packaging*. McGraw-Hill.

12. T. Baumeister, editor. 1966. *Standard Handbook for Mechanical Engineers*, 7th Ed., McGraw-Hill Book Co.

13. Thermalloy Inc. Bulletin 79-HS-5, Semiconductor accessories.
14. Copper Development Association, Inc. Alloy data. *Alloy Data 10a*.

Appendix

Solder: 10Sn-88Pb-2Ag (Refs. 10–12)
Specific heat = 0.033 (cal/g°C)
Density = 10.9 (g/cm^3)
Thermal conductivity = 0.0868 (cal/cm s°C)
Melting point = 320°C
Boiling point = 1740°C

Alumina: 94% nominal Al_2O_3 (Ref. 13)
Specific heat = 0.21 (cal/g°C) at 100°C
Density = 3.62 (g/cm^3)
Thermal conductivity = 0.029 (cal/cm s°C) at 200°C

Beryllia: 99.5% minimum BeO (Ref. 13)
Specific heat = 0.25 (cal/g°C)
Density = 2.85 (g/cm^3)
Thermal conductivity = 0.35 (cal/cm s°C) at 150°C

Terminal lead: SAE CA 260 Brass (70 Cu = 30Zn) (Ref. 14)
Specific heat = 0.09 (cal/g°C) at 20°C
Density = 8.53 (g/cm^3) at 20°C
Thermal conductivity = 0.29 (cal/cm s°C) at 20°C
Melting point = 955°C

Correction

Figure 13, on page 248-s of the August 1987 *Welding Journal* Research Supplement, published as part of the article entitled "An Investigation of Weld Hot Cracking in Duplex Stainless Steels," by D. E. Nelson, W. A. Baeslack III and J. C. Lippold, omitted the following tabular material:

	Nominal Composition	FZ Matrix (Ferrite) (4)	FZ Grain Boundary (Austenite) (3)	Hot Crack Tip (Austenite) (1, 2)
Chromium	24.90	25.94	25.79	25.32
Silicon	0.54	0.42	0.45	0.61
Manganese	1.05	1.08	1.24	1.42
Nickel	5.39	5.27	6.26	8.17
Molybdenum	3.13	3.30	2.80	3.65
Copper	1.72	1.51	1.80	2.50
Phosphorus	0.023	0.03	0.03	0.11
Sulfur	0.001	0.04	0.04	0.06

This table was intended to be used for reference to describe the photograph that was published as Fig. 13.

WRC Bulletin 324
June 1987

Investigation of Design Criteria for Dynamic Loads on Nuclear Power Piping
By R. J. Scavuzzo and P. C. Lam

The objective of this report was to present the experimental work on 304 Stainless Steel Schedule 40 pipes and to evaluate the ability of finite element programs to predict measured responses. Finite element analyses and measured data were also compared to closed form functional solutions. Results of the study indicated that the piping neither damaged nor showed evidence of large plastic deformation, although the code dynamic allowable stress limit was exceeded.

Publication of this report was sponsored by the Subcommittee on Dynamic Analysis of Pressure Components of the Pressure Vessel Research Committee of the Welding Research Council. The price of WRC Bulletin 324 is $16.00 per copy, plus $5.00 for postage and handling. Orders should be sent with payment to the Welding Research Council, Suite 1301, 345 E. 47th St., New York, NY 10017.